Electronic Supplementary Information

Highly selective and ultrafast uptake of uranium from seawater by layered double hydroxide co-intercalated with acetamidoxime and carboxylic anions

Qian Wang,[a] Hui Wang,[a] Lixiao Yang,[a] Huiqin Yao,[b,*] Zhenglong Wu,[c,*] Tao Yu,[d,*] Keren Shi,[e] Shulan Ma[a,*]

[a] Beijing Key Laboratory of Energy Conversion and Storage Materials, College of Chemistry, Beijing Normal University, Beijing 100875, China. E-mail: mashulan@bnu.edu.cn

[b] School of Basic Medical Sciences, Ningxia Medical University, Yinchuan 750004, China. E-mail: huiqin_yao@163.com

[c] Analytical and Testing Center, Beijing Normal University, Beijing 100875, China. E-mail: wuzl@bnu.edu.cn

[d] Third Institute of Oceanography, Ministry of Natural Resource, Xiamen 361005, China. E-mail: yutao@tio.org.cn.

[e] State Key Laboratory of High-efficiency Utilization of Coal and Green Chemical Engineering, Ningxia University, Yinchuan 750021, China.

Supplementary Note 1. Chemicals and materials

Magnesium nitrate ($Mg(NO_3)_2·6H_2O$, Tianjin Damao Chemical Reagent Co., Ltd, 99.0%), aluminium nitrate ($Al(NO_3)_3·9H_2O$, Sinopharm Chemical Reagent Co., Ltd, 99.0%), barium acetate (C_2H_5ONa, Xilong Scientific Co., Ltd. ≥99.0%), acetamidoxime ($C_2H_6N_2O$, Bide Pharmatech Co., Ltd, >97.0%), uranyl nitrate ($UO_2(NO_3)_2·6H_2O$, Shanghai Acmec Biochemical Co., Ltd, 99%), formamide (CH_3NO, Xilong Scientific Reagent Co., Ltd, 99.0%). All solvents and chemical regents in the present work were of analytical reagents and were used without further purification. And deionized water was used in all experiments.

Supplementary Note 2. Characterization Techniques

Fourier-transform infrared (FT−IR) spectra were recorded with a Nicolet-380 FT−IR spectrometer using the KBr pellet method. X-ray diffraction (XRD) was performed on a PANalytical X'pert Pro MPD diffractometer with Cu-Kα radiation at room temperature, with step size of 0.0334°, scan time 20 s per step, and 2θ ranging from 5 to 80°. The morphology of the samples were characterized with scanning electron microscope (SEM) on a Hitachi S-4800 microscope. The solid samples after the adsorption experiments were performed by X-ray photoelectron spectroscopy (XPS) using an ESCALAB 250Xi spectrometer (Thermofisher). The peaks were fitted using the software Avantage.

The metal ion concentrations in supernatant solutions before and after adsorptions were analyzed using the inductively coupled plasma atomic emission spectrometer (ICP-AES, Jarrel-ASH, ICAP-9000) and inductively coupled plasma mass spectrometry (ICP-MS, PE, NEXION300X), respectively. The concentrations of the anions in solutions before adsorption were analyzed using the ion chromatography (IC, ICS-1100). Photon correlation spectroscopy (PCS, Nanosizer Nano ZS, Malvern

Instruments) was used to analyze the particle size distribution of the LDH suspensions. Zeta potentials of the two diluted LDH suspensions were also measured using the Zetasizer Nano ZS (Malvern Instruments). The metal ion contents in solid samples were determined by ICP-AES, and a 0.1 M HNO_3 solution was used to dissolve them. The contents of C, H and N in solid samples were determined by Elementar Vario EL elemental analyzer. The chemical formulas of the samples were determined from the results of ICP and CHN elemental analyses. A Sartorius universal type pH meter (PB-10) was used to monitor the pH value of the solutions before and after adsorption.

Supplementary Note 3. The demonstration of hydrolysis of formamide

To check whether the ultrasound treatment of FM with NaOH can make the hydrolysis of FM to produce formate or methanoate anions, we have carried out some complementary experiments. In brief: 0.075 g of NaOH was dissolved in 1 mL of FM with ultrasound treatment for complete dissolution, kept standing for 24 h at room temperature. Ensure that all experimental parameters and conditions are the same as the synthesis process of ACAO-AC-LDH. To allow the unreacted FM to evaporate, the obtained solution (*abbr.* FM + NaOH) was dropped onto KBr pieces and left at room temperature for 24 hours to test the FT-IR spectra, as shown in Fig. S2 A-b. † By comparing the FT-IR of FM and FM + NaOH, it can be seen that FM surely hydrolyzes to form formate anions under ultrasound treatment with NaOH.

To further determine the degree of FM hydrolysis and the influence of FM hydrolysis on the composition of ACAO-AC-LDH, we supplemented the experiments to synthesize LDH composite, without adding ACAO organic only adding FM and NaOH. In brief: 0.1 g of NO_3-LDH was dispersed into 20 mL of FM, forming a colloidal suspension. Simultaneously, 0.075 g of NaOH was dissolved in 20 mL of FM with ultrasound treatment for complete dissolution. Then the two solutions were mixed and

kept standing for 24 h at room temperature. Ensure that all experimental parameters and conditions are the same as the synthesis procedures of ACAO-AC-LDH. The FT-IR of the formed LDH composite are shown in Fig. S2 A-c. † From Fig. S2 A-c, † FM hydrolyzes to form formate anions under ultrasound treatment with NaOH and the formate anions produced by FM hydrolysis were inserted into the LDH layer to synthesize LDH-formate composite. In the revised manuscript, we added formate anions into the composition formula of ACAO-AC-LDH, got the new composition formula of $Mg_{0.66}Al_{0.34}(OH)_2(C_2H_5N_2O)_{0.03}(C_2H_3O_2)_{0.08}(CHO_2)_{0.01}(CO_3)_{0.11}\cdot H_2O$ (Table S1†), in which the quality fraction of formate anions is only 0.49 percent (=45×0.01/91.202, M_{CHO2}=45, $M_{ACAO\text{-}AC\text{-}LDH}$ = 91.202), we can know that the degree of FM hydrolysis is too low to have obvious effect on the composition of ACAO-AC-LDH.

In order to determine the influence of FM hydrolysis on the adsorption performance of ACAO-AC-LDH, we supplemented the experiments to explore adsorption property of LDH-formate composite. We found at low concentration (10 ppm), the adsorption performance of LDH-formate was good with a removal rate of 99.57 %, while at high concentration (500 ppm), that was only 14 % and the adsorption capacity was ~70 $mg\cdot g^{-1}$, just a little bit higher than that (~20 $mg\cdot g^{-1}$) of NO_3-LDH precursor. We can speculate that formate anions produced by the hydrolysis of FM have no obvious effect on the adsorption performance of ACAO-AC-LDH.

To sum up, though FM surely would hydrolyze to form formate anions under ultrasound treatment with NaOH, the degree of FM hydrolysis is too low to have obvious effect on the adsorption performance of ACAO-AC-LDH. Therefore, we mainly considered the contribution of acetamidoxime and its hydrolysate of acetate anions for U adsorption in this work.

Supplementary Note 4. The demonstration of hydrolysis of acetamidoxime

In order to further affirm that ACAO can hydrolyze to form acetate ions under alkaline conditions, we have designed two experiments. In brief: 0.075 g of NaOH and 0.28 g of ACAO were dissolved in 1 mL of deionized water and 1 mL of ethanol (C_2H_6O), respectively, with ultrasound treatment and kept standing for 24 h at room temperature. Ensure that all experimental parameters and conditions are the same as the synthesis process of ACAO-AC-LDH. To allow the deionized water and ethanol solvents to evaporate, the obtained solutions (*abbr.* ACAO + NaOH + H_2O and ACAO + NaOH + C_2H_6O, respectively) were dropped onto KBr pieces and left at room temperature for 24 h to test the FT-IR spectra, as shown in Fig. S2 B-b, † and Fig. S2 B-c, †, respectively. Comparing with the FT-IR spectra of pure ACAO (Fig. S2 B-a†), it can be seen that A ACAO surely hydrolyzes to form acetate anions under ultrasound treatment with NaOH, though in different solvents.

Supplementary Note 5. The significance of the hydrolysis of acetamidoxime

For the purpose of verifying whether the hydrolysis of ACAO has an advantage for the U(VI) adsorption performance, we have conducted the experiments to explore the significance of the hydrolysis of ACAO.

Firstly, single acetamidoxime (ACAO) is intercalated into MgAl-LDH interlayers to generate a new material of ACAO-LDH via the swelling/restoration reaction. In brief, 0.28 g (3.78 mmol) of ACAO was dissolved in 20 mL of FM with ultrasound treatment for complete dissolution. Other procedures were the same as the synthesis of ACAO-AC-LDH composites. And single acetate anions (Ac^-) are intercalated into MgAl-LDH interlayers to generate a new material of AC-LDH via the swelling/restoration reaction. In brief, 0.31 g (3.78 mmol) of NaAc was dissolved in 20 mL of FM with ultrasound treatment for complete dissolution. Other procedures were the same as the synthesis of

AC-LDH composites. The FT-IR and XRD of the ACAO-LDH and AC-LDH composite are shown in Fig. S3. † The above XRD and FT-IR results show that $ACAO^-$ and Ac^- were exchanged with NO_3^- into the LDH layers, respectively, the ACAO-LDH and AC-LDH composites were successfully obtained via the swelling/restoration reaction. Besides, from Fig. S3, † the 1.14 nm of the d_{basal} of ACAO-LDH (Fig. S3 A-b†) and the 0.98 nm of the d_{basal} of AC-LDH (Fig. S3 A-c†) respectively correspond to the 1.12 nm and 0.97 nm of d_{basal} of ACAO-AC-LDH (Fig. S3 A-a†), and the 0.78 nm of the d_{basal} of LDH-formate (Fig. S3 A-d†) do not correspond to the d_{basal} of ACAO-AC-LDH, which further proves that the main guests in LDH layers are acetamidoxime and its hydrolysate of acetate anions.

Secondly, the experiments of maximum uptake capacity and adsorption kinetics of ACAO-LDH and AC-LDH were implemented, respectively, the procedures were the same as the above experiments of ACAO-AC-LDH composites, and the results are listed in Fig. S4, † and Fig. S5, † respectively.

Similar to ACAO-AC-LDH, the adsorption for U(VI) by ACAO-LDH and AC-LDH are found to fit the Langmuir model and the pseudo-second-order model well. Differently, ACAO-LDH (214 $mg \cdot g^{-1}$) and AC-LDH (175 $mg \cdot g^{-1}$) have a smaller $q_m{}^U$ than ACAO-AC-LDH (339 $mg \cdot g^{-1}$). And ACAO-LDH ($k_2 = 0.0027$ $g \cdot mg^{-1} \cdot min^{-1}$) and AC-LDH ($k_2 = 0.0021$ $g \cdot mg^{-1} \cdot min^{-1}$) have a slower adsorption rate than ACAO-AC-LDH ($k_2 = 3.06$ $g \cdot mg^{-1} \cdot min^{-1}$). The above experimental results show that both ACAO-LDH composite introduced by single ACAO organic guest and AC-LDH composite inserted by single Ac^- organic guest have poor U(VI) adsorption performance than ACAO-AC-LDH composite co-intercalated by the two guests of $ACAO^-$ and Ac^-.

To sum up, the hydrolysis of ACAO is conducive to the adsorption of uranium. The reason may be the common presence of amidoxime and carboxylic would contribute

greatly to increase the adsorption performance, which may be due to the synergistic effect between $ACAO^-$ and Ac^- for U(VI) absorption make free standing amidoxime and carboxyl groups in the LDH layers hold significant affinity towards U(VI).

Supplementary Note 6. Solubility of ACAO-AC-LDH in wide pH solutions.

We immersed 0.02 g of ACAO-AC-LDH, containing 3.5 mg of Mg and 2.0 mg of Al based on the composition of $Mg_{0.66}Al_{0.34}(OH)_2(C_2H_5N_2O)_{0.03}(C_2H_3O_2)_{0.08}(CHO_2)_{0.01}(CO_3)_{0.11}\cdot H_2O$, in 20 mL deionized water at pH values of 4, 5, 7 and 10, and kept standing for 24 h at room temperature. We found that at pH = 5, the average concentration of Mg was 25 $mg\cdot L^{-1}$ and that of Al was 0.04 $mg\cdot L^{-1}$ in 20 mL solution, corresponding to 0.50 mg of Mg and 0.0008 mg of Al. Therefore, the dissolved mass fraction of Mg was 14.29% and that of Al was 0.04%. Similarly, at pH of 4, 7 and 10, the dissolved mass fraction of Mg was 16.00%, 9.14% and 6.86%, respectively, the dissolved mass fraction of Al was 0.05%, 0.02% and 0.01%, respectively. To sum up, in the acidic, neutral and basic solutions, the ACAO-AC-LDH material will dissolve slightly to some extent, especially in the weak acid solution.

Supplementary Note 7. Related calculations and formulas

7.1 Langmuir adsorption isotherm models:

$$q = q_m \frac{bC_e}{1 + bC_e} \quad \text{(Eq. 1)}$$

$$\frac{C_e}{q_e} = \frac{C_e}{q_m} + \frac{1}{q_m K_L} \quad \text{(Eq. 2)}$$

Where q ($mg\cdot g^{-1}$), q_m ($mg\cdot g^{-1}$), C_e ($mg\cdot L^{-1}$) and K_L ($L\cdot mg^{-1}$) are the equilibrium adsorption capacity, theoretical maximum adsorption capacity, equilibrium concentration and Langmuir constant, respectively.

7.2 Pseudo-first-order and pseudo-second-order dynamic models:

pseudo-first-order:

$$\ln (q_e - q_t) = \ln q_e - k_1 t \qquad \text{(Eq. 3)}$$

pseudo-second-order:

$$\frac{t}{q_t} = \frac{1}{k_2 q_e^2} + \frac{t}{q_e} \qquad \text{(Eq. 4)}$$

where q_e (mg·g^{-1}): equilibrium adsorption capacity of unit mass, q_t (mg·g^{-1}): adsorption capacity at time of t, k_1 (min^{-1}) and k_2 (g·mg^{-1}·min^{-1}): equilibrium rate constants, and k_1 and k_2 can be getted by ln(q_e-q_t) and t/q_t, respectively.

7.3 Distribution coefficient (K_d):

$$K_d = (V[(C_0 - C_f)/C_f])/m \qquad \text{(Eq. 5)}$$

where V is the solution volume (mL), and m is the adsorbent quality (g), C_0 and C_f are initial and equilibrium concentration of the ions (μg/mL).

Supplementary Note 8. The reasons why organic ligands should not leave the interlayer region after ACAO-AC-LDH adsorbed U(VI)

When ACAO-AC-LDH material adsorbed UO_2^{2+}, NO_3^- anions would accompany with UO_2^{2+} into the interlayer of LDH to balance the charge. But the organic ligands should not leave the interlayer region. Five reasons are as follows: (i) the hydrogen bonding between -NH_2 of ACAO-U(VI) complex and LDH hydroxyls (-OH) also promoted the structural stability; (ii) the dimensions of the organic ligands-U(VI) complex is so large that it is difficult to move between layers. In contrast, the smaller NO_3^- anions will move faster and easier in the solution, so they will be more likely to enter into the LDH layers to balance the charges; (iii) In FT-IR spectra of all post-adsorption samples (Fig. 4A), the existence of 1587, 1381 and 1071 cm^{-1} bands assigned to ν_a(C=N), ν_s(−COO$^-$) and

ν(C-N), respectively, further shows the organic ligands-U(VI) complex still exists in the layer. And comparing macroscopically the FT-IR spectra of NO_3-LDH, ACAO-AC-LDH and the post-adsorption samples, the FT-IR spectra of ACAO-AC-LDH and the post-adsorption samples are similar, and the difference between NO_3-LDH and the post-adsorption samples is obvious; (iv) If the organic ligands-U(VI) complex have left the interlayer region, the post-adsorption samples will be NO_3-LDH and the d_{basal} values of all post-adsorption samples will be 0.90 nm, not gradually increase. So the XRD patterns of U-adsorbed samples (Fig. 4B) also show that organic ligands-U(VI) complex has not left the layers; (v) The ACAO-U(VI) complex is soluble in water. If organic ligands have left the layers, the organic ligands-U(VI) complex also existed in the aqueous solution, so U(VI) cannot be effectively separated from aqueous solution, which is inconsistent with the results of the experiments.

Table S1. Composition of the ACAO-AC-LDH composite.

Chemical formula	wt%, found (calcd)				
	Mg	Al	C	H	N
$Mg_{0.66}Al_{0.34}(OH)_2(C_2H_5N_2O)_{0.03}(C_2H_3O_2)_{0.08}(CHO_2)_{0.01}(CO_3)_{0.11}\cdot H_2O$	17.32	9.89	4.59	4.39	0.79
	(17.59)	(10.07)	(4.47)	(4.82)	(0.92)

The found data (experimental data) were obtained by CHN and ICP, and the calcd data (theoretical data) were determined based on the chemical formula.

Table S2. Adsorption data of ACAO-AC-LDH at 109 ppm U(VI) at different pH. [a)]

C_0 (ppm)	pH	C_f (ppm)	q_m (mg·g^{-1})	Removal (%)
109	4.05→5.25	22.2	86.8	79.63
	4.99→8.45	7.25	101.75	93.35
	5.96→6.65	20.5	88.5	81.19
	7.03→6.40	11.5	97.5	89.45
	7.95→9.20	9.58	99.42	91.21
	8.98→9.10	17.4	91.6	84.04

9.97→7.80	24.5	84.5	77.52

[a)] m = 0.02 g, V = 20 mL, V/m = 1000 mL·g^{-1}; contact time: 24 h.

Table S3. Parameters for pseudo-second-order dynamic model of U(VI) sorption on ACAO-AC-LDH.

$q_{e,\,exp}$ (mg·g^{-1})	k_2	$q_{e,\,cal}$ (mg·g^{-1})	R^2
12.75	3.06	12.75	1

Table S4. Adsorption of ACAO-AC-LDH toward mixed ions.[a)]

Ions	C_0 (ppm)	C_f (ppm)	Uptake (%)	K_d (mg/L)	SF_U^M
Ca^{2+}	9.87	9.54	3.34	34.6	2.84×10^5
Mg^{2+}	10.3	9.31	9.61	106	9.25×10^4
K^+	9.68	9.42	2.69	27.6	3.56×10^5
Na^+	9.72	9.62	1.03	10.4	9.43×10^5
UO_2^{2+}	9.81	0.001	99.9	9.81×10^6	-

a) m = 0.02 g, V= 20 mL, V/m = 1000 mL·g^{-1}. pH: 4.23→9.10.

Table S5 Adsorption of UO_2^{2+} with Cl^-, SO_4^{2-}, NO_3^-, HCO_3^- and CO_3^{2-} by ACAO-AC-LDH. [a)]

Mixed ions	C_0 (ppm)	C_f^U (ppm)	Removal of U (%)	K_d^U (mL g^{-1})
UO_2^{2+} Cl^- [b)]	9.88 17601	≤0.001	≥99.99	9.88×10^6
UO_2^{2+} SO_4^{2-} [c)]	10.02 2664	0.003	99.97	3.34×10^6
UO_2^{2+} NO_3^- [d)]	9.66 10.2	≤0.001	≥99.99	9.66×10^6
UO_2^{2+} HCO_3^- [e)]	10.00 147	0.001	99.99	10.0×10^6
UO_2^{2+} CO_3^{2-} [f)]	9.89 10.0	≤0.001	≥99.99	9.89×10^6

[a)] m = 0.02 g, V= 20 mL, V/m = 1000 mL·g^{-1}. pH: [b)] 6.42→7.10; [c)] 6.38→7.21; [d)] 6.55→7.14; [e)] 8.55→8.71; [f)] 8.10→8.34.

Table S6 Desorbed results for U(VI)-adsorbed sample (q_m=302.1 mg·g^{-1}) using $NaNO_3$ and HNO_3 as eluents.

	$NaNO_3$	HNO_3
C-eluent (mg·L^{-1})	2.34	25.8
q_m (mg·g^{-1}) in sorption	302.1	302.1
Desorption efficiency (%) [a)]	0.77	8.54

[a)] Calculation of desorption efficiency, for example, when using $NaNO_3$ as eluent: (2.34 mg·L^{-1} × 0.005 L)/(302.1 mg·g^{-1} × 0.005 g) ×100% = 0.77%.

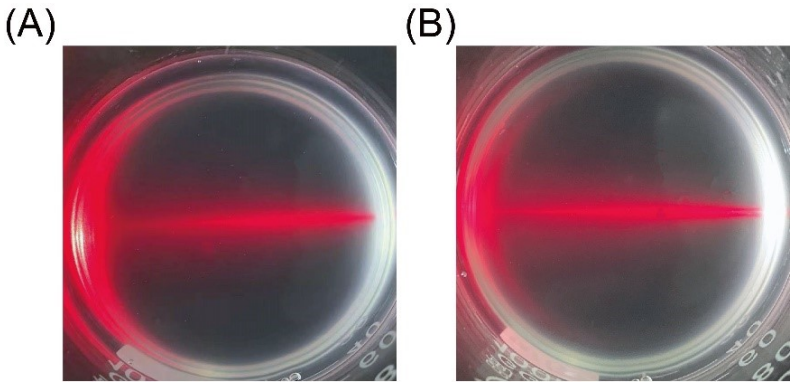

Fig. S1 Tyndall light scattering of colloidal suspension of (A) NO_3-LDH in formamide and (B) ACAO-AC-LDH in formamide.

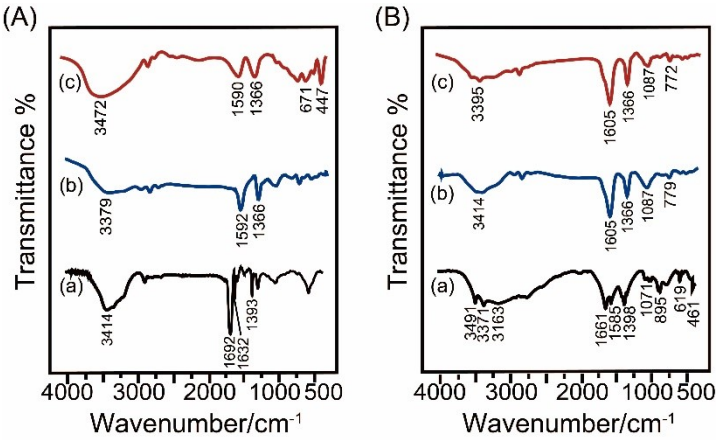

Fig. S2 (A) FT-IR spectra of (a) FM, (b) FM + NaOH and (c) LDH-formate; (B) FT-IR spectra of (a) ACAO, (b) ACAO + NaOH +H_2O and (c) ACAO + NaOH + C_2H_6O.

From Fig. S2 A-b, † the bands at 1592 and 1366 cm^{-1} could be ascribed to $\nu_a(-COO^-)/\nu_s(-COO^-)$, verifying the presence of $-COO^-$ groups. For pure FM (Fig. S2 A-a†), the bands at 1692, 1632 and 1393 cm^{-1} could be ascribed to ν(C=O), $\delta(NH_2)$ and ν(C-N), respectively.

From Fig. S2 A-c, † the 1590 and 1366 cm^{-1} bands could be ascribed to $\nu_a(-COO^-)/\nu_s(-COO^-)$ and the 671 and 447 cm^{-1} bands were ascribed to ν(M-O) and δ(O-M-O) vibrations of LDH layers.

For ACAO + NaOH + H_2O (Fig. S2 B-b†) and ACAO + NaOH + C_2H_6O (Fig. S2 B-c†), the bands at 1605 and 1366 cm^{-1} could be ascribed to $\nu_a(-COO^-)/\nu_s(-COO^-)$, verifying the presence of $-COO^-$ groups.

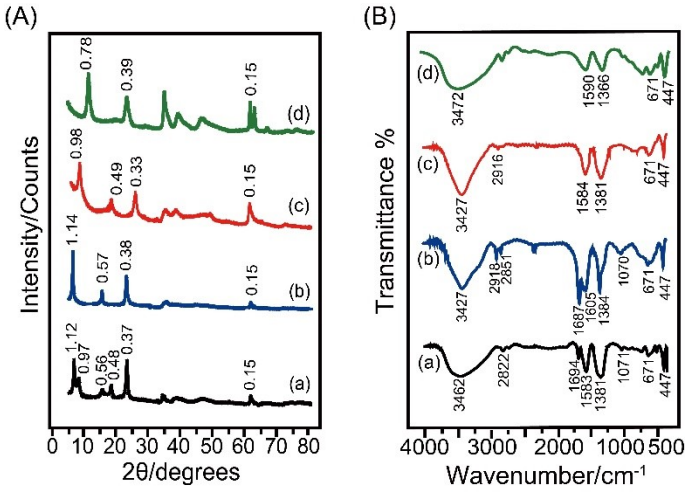

Fig. S3 (A) XRD patterns and (B) FT-IR spectra of (a) ACAO-AC-LDH composite, (b) ACAO-LDH composite, (c) AC-LDH composite and (d) LDH-formate.

From the XRD patterns of ACAO-LDH (Fig. S3 A-a†), the enlarged d_{basal} values of 1.14 nm suggests $ACAO^-$ guests have entered the LDH gallery and replaced original NO_3^-. From the FT-IR spectra of ACAO-LDH (Fig. S3 B-a†), the 1384 cm^{-1} band is ascribed to the absorptions NO_3^-, and the 1687, 1605 and 1071 cm^{-1} bands are respectively assigned to ν_a(C=N), ν_s(C=N) and ν(C-N). The blue shift of the ν_a(C=N) (from 1661 to 1687 cm^{-1}) and ν_s(C=N) (from 1585 to 1605 cm^{-1}) indicates that

enhanced C=N bonding in the ACAO-LDH composite. From the XRD patterns of ACAO-LDH composite (Fig. S3 A-b†), the enlarged d_{basal} values of 1.14 nm suggests $ACAO^-$ guests have entered into the LDH gallery and replaced original NO_3^- anions. From the FT-IR spectra of ACAO-LDH composite (Fig. S3 B-b†), the 1384 cm^{-1} band is ascribed to the absorptions NO_3^-, the 1687, 1605 and 1071 cm^{-1} bands are respectively assigned to ν_a(C=N), ν_s(C=N) and ν(C-N). The blue shift of the ν_a(C=N) (from 1661 to 1687 cm^{-1}) and ν_s(C=N) (from 1585 to 1605 cm^{-1}) bands indicates that enhanced C=N bonding in the ACAO-LDH composite, ordinating from the deprotonation of -OH of ACAO resulting in the increased electron density of $-O^-$, thus further leading to the increase of the electron density of the connected N. The obtained AC-LDH powder exhibits an enlarged d_{basal} of 0.98 nm (Fig. S3 A-c†), demonstrating that bulk Ac^- guests have been introduced into the LDH interlayers. In the FT-IR spectra of AC-LDH composite (Fig. S3 B-c†), the two bands at 1584 and 1381 cm^{-1} respectively ascribed to $\nu_a(-COO^-)/\nu_s(-COO^-)$.

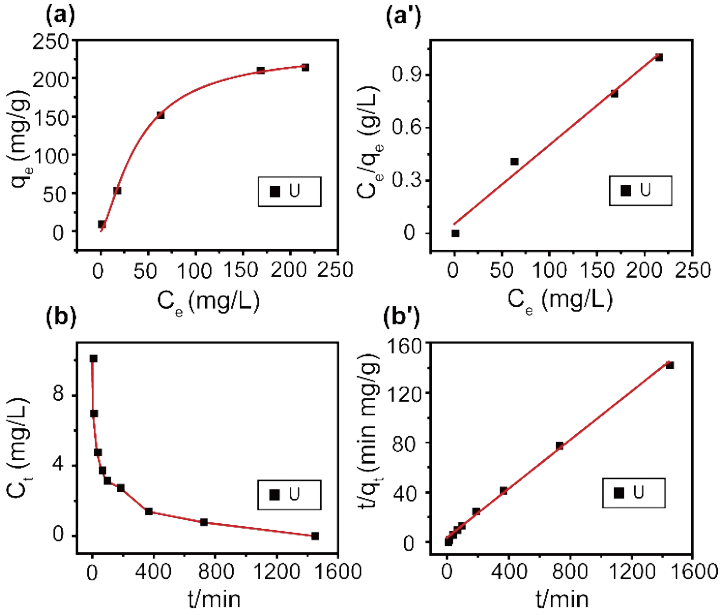

Fig. S4 (a, a') Langmuir equilibrium isotherms of U(VI) sorption by ACAO-LDH derived from equilibrium concentration (C_e, mg/L) plotted against q_e (mg/g) and C_e/q_e

(g/L), and (b, b') sorption kinetics curves of U(VI) by ACAO-LDH: (b) U concentration (C_t) change with contact time, (b') pseudo-second-order kinetic plot.

The adsorption for U(VI) by ACAO-LDH (Fig. S4 a, a'†) is found to fit the Langmuir model well, giving the R^2 of ACAO-LDH are 0.99 and 0.98. In ACAO-LDH, the calculated q_m^U of 237 and 222 mg·g^{-1} are also much close to the experimental value of 214 mg·g^{-1}. And the t/q_t has a linear relationship with t in Fig. S4 b', † the theoretical equilibrium adsorption capacity (the $q_{e,cal}$ is 10.17 mg·g^{-1}) from the pseudo-second-order model is equal to the experimental value (the $q_{e,exp}$ is10.1 mg·g^{-1}) and the high R^2 of pseudo-second-order kinetics (the R^2 is 0.99) suggest that the adsorption process for U(VI) by ACAO-LDH belong to the pseudo-second-order model.

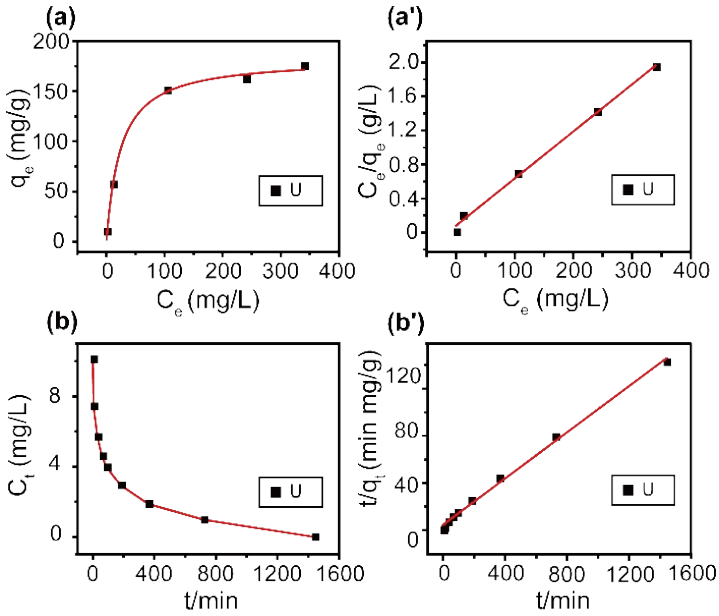

Fig. S5 (a, a') Langmuir equilibrium isotherms of U(VI) sorption by AC-LDH derived from equilibrium concentration (C_e, mg/L) plotted against q_e (mg/g) and C_e/q_e (g/L), and (b, b') sorption kinetics curves of U(VI) by AC-LDH: (b) U concentration (C_t) change with contact time, (b') pseudo-second-order kinetic plot.

The adsorption for U(VI) by AC-LDH (Fig. S5 a, a'†) is found to fit the Langmuir model well, giving the R^2 of AC-LDH are 0.99 and 0.99. In AC-LDH, the calculated q_m^U of 182 and 180 mg·g^{-1} are also much close to the experimental value of 175 mg·g^{-1}.

And the t/q_t has a linear relationship with t in Fig. S5 b'†, the theoretical equilibrium adsorption capacity (the $q_{e,cal}$ of AC-LDH is 10.20 mg·g^{-1}) from the pseudo-second-order model is equal to the experimental value (the $q_{e,exp}$ of AC-LDH is 10.1 mg·g^{-1}) and the high R^2 of pseudo-second-order kinetics (the R^2 is 0.99) suggest that the adsorption process for U(VI) by AC-LDH belong to the pseudo-second-order model.

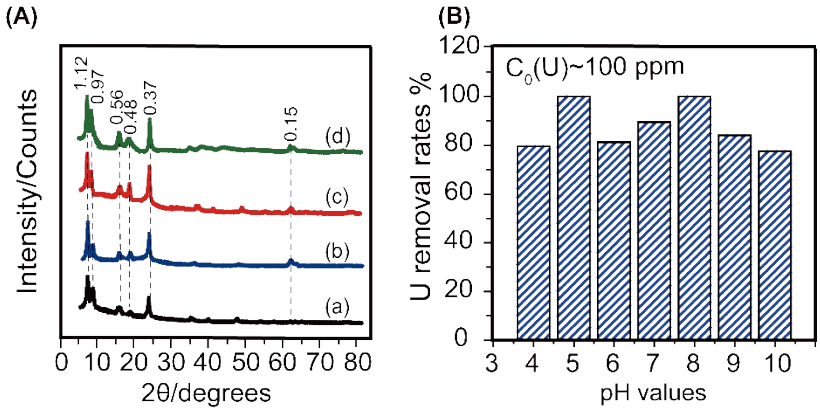

Fig. S6 (A) XRD patterns of post-immersion samples of ACAO-AC-LDH composite in deionized water of (a) pH=4, (b) pH=5, (c) pH=7 and (d) pH=10; (B) Effect of pH on U adsorption by ACAO-AC-LDH.